BJP British Journal of Pharmacology

DOI:10.1111/bph.12778
www.brjpharmacol.org

RESEARCH PAPER

Inhibitory role of phosphatidylinositol 4,5-bisphosphate on TMEM16A-encoded calcium-activated chloride channels in rat pulmonary artery

H A T Pritchard[1], N Leblanc[2], A P Albert[1] and I A Greenwood[1]

[1]*Vascular Biology Research Centre, Institute of Cardiovascular and Cell Sciences, St George's, University of London, London, UK, and* [2]*Department of Pharmacology/MS 573, University of Nevada School of Medicine, Reno, NV, USA*

Correspondence
Iain A. Greenwood, Vascular Biology Research Centre, Institute of Cardiovascular and Cell Sciences, St George's, University of London, London SW17 0RE, UK. E-mail: i.greenwood@sgul.ac.uk

Received
21 February 2014
Revised
22 April 2014
Accepted
7 May 2014

BACKGROUND AND PURPOSE

Calcium-activated chloride channels (CaCCs) are key depolarizing mechanisms that have an important role in vascular smooth muscle contraction. Here, we investigated whether these channels are regulated by phosphatidylinositol (4,5) bisphosphate [$P(4,5)P_2$], a known regulator of various ion channels.

EXPERIMENTAL APPROACH

Calcium-activated Cl^- currents (I_{ClCa}) were recorded by patch clamp electrophysiology of rat isolated pulmonary artery smooth muscle cells. TMEM16A protein-phosphoinositide interaction was studied by co-immunoprecipitation and phosphoinositide binding arrays on protein lysates from whole pulmonary arteries and HEK293 cells overexpressing TMEM16A, the molecular correlate.

KEY RESULTS

$PI(4,5)P_2$ and other phospholipids were shown to bind directly to TMEM16A isolated from whole pulmonary artery (PA) and TMEM16A-eGFP expressed in HEK293 cells. Agents that reduced $PI(4,5)P_2$ levels through different routes [PLC activation, PI4K inhibition, $PI(4,5)P_2$ scavenging and absorption] all increased I_{ClCa} evoked by solutions containing clamped-free [Ca^{2+}], whereas enrichment of activating solutions with $PI(4,5)P_2$ inhibited I_{Clca} in PA smooth muscle cells with approximately 50% reduction at 1 μM.

CONCLUSIONS AND IMPLICATIONS

These data are the first to show a negative regulation of TMEM16A-encoded CaCCs by $PI(4,5)P_2$ and propose that control of $PI(4,5)P_2$ levels is a key determinant of arterial physiology.

Abbreviations

CaCC, calcium-activated chloride channel; PASMC, pulmonary artery smooth muscle cells; $P(4,5)P_2$, phosphatidylinositol (4,5) bisphosphate; $T16A_{inh}$-AO1, aminophenylthiazole

Introduction

Stimulation of Ca^{2+}-activated Cl^- channels (CaCCs) has been implicated in a number of physiological processes. In vascular smooth muscle, CaCCs provide a depolarizing mechanism because these cells actively accumulate Cl^- ions through the Na/K/2Cl transporter and the HCO_3/Cl^- exchanger (Chipperfield and Harper, 2000), resulting in a Cl^- equilibrium potential sufficiently more positive than the resting membrane potential to allow Cl^- efflux. As vascular smooth muscle contraction is precipitated by a rise in intracellular Ca^{2+}, principally through Ca^{2+} influx via voltage-dependent Ca^{2+} channels (VDCCs), then CaCC stimulation will increase the likelihood of the VDCCs being open and the concomitant Ca^{2+} influx will enhance vascular contractility. Calcium-activated chloride currents (I_{ClCa}) have been described in vascular smooth muscle cells from a number of different arteries (Greenwood *et al.*, 2001; Angermann *et al.*, 2006; Sones *et al.*, 2010; Dam *et al.*, 2013), and inhibition of the Cl^- accumulation mechanisms or direct block of Cl^- channels by non-specific agents such as niflumic acid attenuates contraction in a number of smooth muscles (Criddle *et al.*, 1996; Yamazaki and Kitamura, 2001). However, the lack of a defined molecular identity for CaCCs has prohibited more precise investigations into the role of CaCCs in vascular physiology and pathophysiology.

Recently, expression products of TMEM16A (anoctamin 1) were shown to comprise native CaCCs (Caputo *et al.*, 2008; Schroeder *et al.*, 2008; Yang *et al.*, 2008) and TMEM16A expression has been identified in various rodent and human arteries (Manoury *et al.*, 2010; Sones *et al.*, 2010; Thomas-Gatewood *et al.*, 2011; Bulley *et al.*, 2012; Wang *et al.*, 2012; Davis *et al.*, 2010; 2013). Reduction of TMEM16A activity either through siRNA, targeted antibodies or use of TMEM16A-specifc pharmacological tools such as aminophenylthiazole ($T16A_{inh}$-AO1) diminishes I_{ClCa} (Manoury *et al.*, 2010; Thomas-Gatewood *et al.*, 2011; Davis *et al.*, 2013) and attenuates vasoconstriction (Dam *et al.*, 2013; Davis *et al.*, 2013), supporting a role for CaCCs in vascular tone. This view is consolidated by the observation that targeted disruption of TMEM16A in vascular smooth muscle cells leads to lower blood pressure and less severe hypertension following angiotensin II infusion (Heinze *et al.*, 2014). Consequently, TMEM16A-encoded CaCCs are key determinants of vascular reactivity, and mechanisms that regulate these channels will have considerable bearing on arterial physiology.

There is growing appreciation that in addition to being a substrate for PLC, phosphatidylinositol (4,5) bisphosphate [$PI(4,5)P_2$] is also a regulator of various ion channels including KCNQ-encoded channels, transient receptor potential channel 1 (TRPC1), K_{ir} and epithelial sodium channels (ENaC) (see Suh and Hille, 2008 for summary; nomenclature conforms to Alexander *et al.*, 2013). However, there is no information about the regulation of CaCCs by $PI(4,5)P_2$. The aim of the present study was to determine, using a combination of different pharmacological reagents, single cell electrophysiology, co-immunoprecipitation and biochemical analysis, whether alterations in $PI(4,5)P_2$ levels affect native I_{ClCa} in rat pulmonary artery smooth muscle cells (PASMCs). Our data revealed that $PI(4,5)P_2$ is a powerful negative regulator of CaCC activity that has considerable implications for cellular physiology.

Methods

Cell isolation

PASMCs were isolated from male Wistar rats (200–225 g), killed in accordance with Schedule 1 of the United Kingdom Animal Acts 1986. The cells were isolated by incubating segments of artery in Ca^{2+}-free physiological salt solution (PSS) containing 0.5 mg·mL^{-1} papain, 1 mM DTT and 2 mg·mL^{-1} BSA overnight at 4°C, followed by trituration through a wide bore glass pipette. Cells were plated on coverslips in PSS, supplemented with 0.75 mM [Ca^{2+}], and experiments were carried out between 1 and 6 h post-seeding. Following the reviewer's comments, a few experiments were performed on cells isolated by a more acute method (1 h in 1.5 mg·mL^{-1} papain at 4°C, then 6 min in 1.5 mg·mL^{-1} papain and 1 mg·mL^{-1} DTT, before being treated with 1.4 mg·mL^{-1} collagenase for 5 min, both at 37°C).

Cell culture and transfection

HEK293 cells were seeded in 6-well plates in MEM, supplemented with 10% FBS, 1% penicillin/streptomycin, 1% non-essential amino acids, 1% sodium pyruvate and 1% L-glutamine. HEK293 cells grown to 70% confluence were transfected with mouse TMEM16A-eGFP ('a' variant) using lipofectamine 2000. Cells were exposed to the plasmid (0.1 μg·cm^{-2}) in antibiotic-free media for 6 h before the medium was replaced with the standard growth media. Cells were then removed with trypsin-EGTA and protein was extracted.

Western blot analysis

Samples of rat pulmonary arteries were homogenized in ice-cold lysis buffer [in mM: 20 Tris base, 137 NaCl, 2 EDTA, 1% nonidet P-40, 10% glycerol (pH 8) and 10 μL·mL^{-1} protease inhibitor cocktail], incubated for 15 min and centrifuged (15 min, 4°C, 9400× *g*). Supernatant was transferred to a separate tube and protein concentration was calculated by the Bradford assay. Knockout samples were a kind gift from Professor Karl Kunzelmann (University of Regensburg, Germany). For each sample, 30 μg of protein was transferred to a PVDF membrane and subjected to analysis using XCell surelock system (Life Technologies, Paisley, UK). Samples were blocked with 5% milk powder in PBS-Tween (0.1%, PBS-T) for 1 h and were probed, overnight at 4°C, with anti-TMEM16A (1:200, ab53212; Abcam, Cambridge, UK), which is the undiluted form of the antibody previously characterized by Davis *et al.* (2010). Excess primary antibody was removed with PBS-T and HRP-conjugated anti-rabbit secondary (1:25 000; Sigma, Poole, Dorset, UK) for 1 h at room temperature (RT). All antibodies were diluted in the milk buffer. Samples were detected with ECL chemiluminescence, exposed to photographic film (both GE Health care, Little Chalfont, UK).

Immunoprecipitation

Immunoprecipitation and dot blots were carried out as described previously (Shi *et al.*, 2014). Whole rat pulmonary

arteries were dissected and treated with either 1 μM U46619 (15 min), 20 μM wortmannin or 3 mg·mL^{-1} α-cyclodextrin (α-CD) (all 1 h). Tissues were lysed and subjected to the same procedure as that used to prepare samples for Western blot analysis. Immunoprecipitation of the rat pulmonary artery was carried out using a Millipore Catch and Release Kit according to the manufacturer's instructions; 400 μg of protein was used per sample and 4 μg of TMEM16A antibody. TMEM16A protein overexpressed in HEK was immunoprecipitated using GFP-Trap_A Kit (Chromotek, Krailling, Germany) according to the manufacturer's instructions, with 400 μg of protein per sample.

Dot blots

Three microlitres of each sample was added to a PVDF membrane and dried, before being blocked in 5% milk powder in PBS-T for 1 h. It was then probed with anti-PI(4,5)P_2 (1:200; Santa Cruz, Heidelberg, Germany) overnight at 4°C, as described previously (Barroso-González *et al.*, 2009; Shi *et al.*, 2014). Excess primary antibody was then removed from the membranes by washing with PBS-T, before the samples were incubated with HRP-conjugated secondary antibody (anti-mouse IgM, 1:2500; Santa Cruz) for 1 h and TMEM16A detected on photographic film as above. Drying the membrane produced dots of various sizes; therefore, the intensities of the dot blots were calculated and normalized to known concentrations of TMEM16A using Image Studio software (LI-COR, Lincoln, NE, USA). Data shown represent findings from at least 3 different animals.

Lipid assay

PIP strips (Life Technologies) were used to test which phospholipids TMEM16A can potentially bind to and experiments were carried out according to the manufacturer's instructions. Briefly, strips were blocked in TBS-Tween (0.1%, TBS-T) and 3% BSA for 1 h. Samples were then diluted in the blocking buffer to 0.5 μg·mL^{-1} and incubated at room temperature for 3 h, washed three times in blocking buffer before the sample was again incubated for another 3 h. Samples were then probed for TMEM16A similar to the dot blot method, but using TBS-T and 3% BSA blocking buffer and detected using Westar Supernova ECL (Geneflow Limited, Lichfield, UK). It is worth stressing that on the PIP strip, although there is 100 pM of lipid in each spot, we did not make comparisons between dot intensities, as they varied in concentration and location due to their physiological nature.

Whole cell recordings

I_{ClCa} was activated by a known amount of 'free' [Ca^{2+}] up to 500 nM, which produced a current immediately upon rupture of the membrane. The pipette solution had the following composition (in mM): TEA (20), CsCl (106), HEPES–CsOH (10, pH 7.2), BAPTA (10), ATP·Mg^{-1} (5) and GTP·diNa^{-1} (0.2). To this solution, 4.2, 6.8 and 7.08 mM $CaCl_2$ were added to achieve free [Ca^{2+}] of 100, 250 and 500 nM respectively (Greenwood *et al.*, 2001; Angermann *et al.*, 2006). The bathing solution had the following composition (in mM): NaCl (126), HEPES–NaOH (10, pH 7.35), TEA (8.4), glucose (20), $MgCl_2$ (1.2) and $CaCl_2$ (1.8). Experiments were carried out under voltage clamp, using protocols described previously (Greenwood *et al.*, 2001; Angermann *et al.*, 2006). Briefly, the 'test' protocol consisted of a step from the holding potential (HP) of −50 to +70 mV and then down to −80 mV before returning to the HP. *I–V* relationships consisted of stepping from the HP to between −100 and +100 mV in 20 mV increments before returning to the HP. Perforated patch recordings were obtained by inclusion of 600 μg·mL^{-1} of amphotericin B in a standard pipette solution. All whole cell recordings were carried out at room temperature.

Single channel recordings

To test the potential role of PI(4,5)P_2 on I_{ClCa} activity, experiments were carried out using the inside-out patch configuration, which enables direct access to intracellular membrane and, therefore, is probably the site of PI(4,5)P_2 interactions. The pipette solution contained (in mM) *N*-methyl-D-glutamine (NMDG-Cl) (126, equimolar addition of NMDG and HCl), $MgCl_2$ (1.2) $CaCl_2$ (10) HEPES (10), pH set at 7.2. The bathing solution (intracellular) contained NMDG-Cl (126), HEPES (10), $MgCl_2$ (1.2), EGTA (0.1) and MgATP (1), pH 7.2 – 64 μM $CaCl_2$ to achieve 500 nM free [Ca^{2+}]. Single channel I_{ClCa} was recorded at room temperature with a HP of −100 mV. Recordings were analysed as shown previously (Piper and Large, 2003; Davis *et al.*, 2013). Briefly, single channel current amplitudes were calculated from traces of at least 60 s in duration using the 50% threshold method.

Statistical analysis

All data are shown as the mean of '*n*' animals ± SEM. After testing for normality, the data were tested for statistical significance using the correct test on GraphPad Prism software (GraphPad Software Inc., San Diego, CA, USA). Whole cell *I–V* relationships and time-course experiments were compared using a two-way ANOVA, with a Bonferroni *post hoc* test at each potential or time period. Single channel relative NP_0 were tested using a paired *t*-test or a Wilcoxon test. Dot blot intensities were compared using a one-way ANOVA, with a Bonferoni *post hoc* test to compare with untreated control.

Materials

$T16_{inh}$-A01 was from Millipore (Watford, UK) and PI(4,5)P_2 was from Echelon Biosciences (Salt Lake City, UT, USA). All other chemicals were purchased from Sigma.

Results

PI(4,5)P_2 is bound to native rat PA TMEM16A at rest

Similar to our previous studies on mouse and rat blood vessels (Davis *et al.*, 2010; Forrest *et al.*, 2012), probing with a TMEM16A-antibody produced a band at about 120 kDa in rat PA protein lysates. In HEK293 cells heterologously expressing eGFP-tagged TMEM16A, the band was slightly higher at about 150 kDa, consistent with the extra molecular weight of the eGFP tag, which is separated from the endogenous TMEM16A within HEK293 cells. (Figure 1Ai). TMEM16A was not detected in kidney lysate from TMEM16A knockout mice,

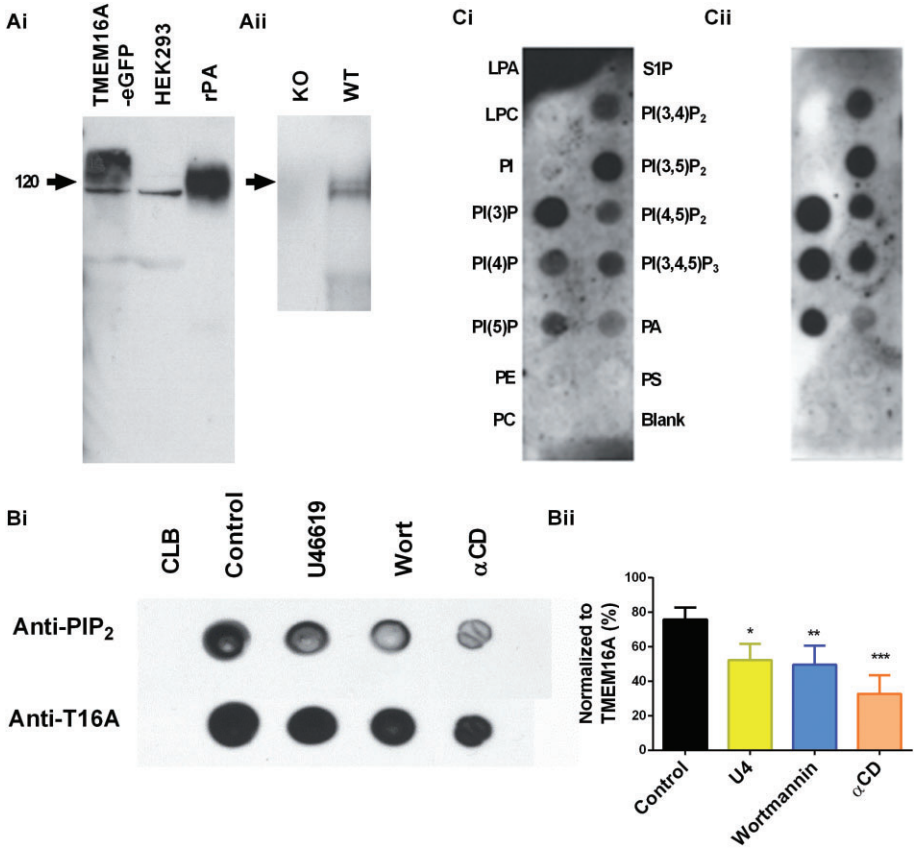

Figure 1

Biochemical analysis of TMEM16A and PI(4,5)P interaction. (A) Western blot analysis of anti-TMEM16A antibody previously characterized by Davis *et al.* (2010) on lysates isolated from HEK293 cells transfected with TMEM16A-eGFP, untransfected HEK293 cells, rat PA and kidney lysates from knockout (KO) and wild-type (WT) mice. (B) Immunodetection of $PI(4,5)P_2$ in rat PA lysates precipitated using TMEM16A antisera in the absence and presence of U46619 (1 μM, 15 min, $*P < 0.05$), wortmannin (20 μM, 1 h, $**P < 0.01$), and αCD (3 mg·mL^{-1}, 1 h, $***P < 0.001$) compared using one-way ANOVA versus control. (Bii) The mean intensity of dots produced by the $PI(4,5)P_2$ antisera normalized to the dot intensity when TMEM16A antisera was used ($n = 3$). (C) PIP strips were used to see the lipid binding potential of purified rat PA TMEM16A. (Ci) Lipids include lysophosphatidic acid (LPA), lysophosphocholine (LPC), phosphatidylinositol (PI), phosphatidylinositol (3) phosphate [PI(3)P], phosphatidylinositol (4) phosphate [PI(4)P], phosphatidylinositol (5) phosphate [PI(5)P], phosphatidylethanolamine (PE), phosphatidylcholine (PC), sphingosine 1-phosphate (S1P), phosphatidylinositol (3,4) bisphosphate [$PI(3,4)P_2$], phosphatidylinositol (3,5) bisphosphate [$PI(3,5)P_2$], phosphatidylinositol (4,5) bisphosphate [$PI(4,5)P_2$], phosphatidylinositol (3,4,5) trisphosphate [$PI(3,4,5)P_3$], phosphatidic acid (PA) and phosphatidylserine (PS). Purified overexpressed TMEM16A-eGFP was tested (Cii), with same lipids as in (Ci).

but was detected in wild-type control animals (Figure 1Aii). This antibody was then used to precipitate out TMEM16A from non-denatured rat PA protein lysate. Incubation of the TMEM16A-immunoprecipiated protein lysates with $PI(4,5)P_2$ antisera produced positive signals consistent with this phospholipid being associated with the channel in rat PA (Figure 1B). Treatment of whole PA with agents that deplete $PI(4,5)P_2$, namely the thromboxane receptor agonist U46619 (1 μM, 15 min), wortmannin (20 μM, 1 h) and αCD (3 mg·mL^{-1}, 1 h), resulted in a reduction in signal intensity produced by the $PI(4,5)P_2$ antisera (Figure 1Bii). Incubation of TMEM16A-precipitated protein lysate with phosphoinositides stabilized onto membrane arrays (so-called 'PIP strips') showed that TMEM16A from the rat PA bound phosphatidic acid and all phosphatidylinositols (PI) including $PI(4,5)P_2$ (Figure 1Ci). We repeated these studies using overexpressed TMEM16A-eGFP protein, which was purified using a GFP-Trap kit (Chromotek) and its lipid binding profile was similar to that of native TMEM16A (Figure 1Cii).

Enrichment with $PI(4,5)P_2$ attenuated I_{Clca}

Having established that TMEM16A and $PI(4,5)P_2$ interact physically, we investigated what effect $PI(4,5)P_2$ had on native Ca^{2+}-dependent Cl^- currents (I_{Clca}) in rat PA smooth muscle cells. Consistent with previous experiments in this artery (Forrest *et al.*, 2012; Sun *et al.*, 2012) and other vascular smooth muscle cells (Greenwood *et al.*, 2001; Angermann *et al.*, 2006; Sones *et al.*, 2010; Davis *et al.*, 2013), I_{ClCa} were evoked immediately after the pipette solutions containing [Ca^{2+}] at fixed levels of 100, 250 or 500 nM gained access to the whole cell, which exhibited distinctive voltage-dependent kinetics (Figure 2Ai,Aii). These currents were inhibited by the TMEM16A-specific blocker $T16A_{inh}$-AO1 (Figure 2Aiii; $n = 4$, $P < 0.001$) to an extent comparable to that

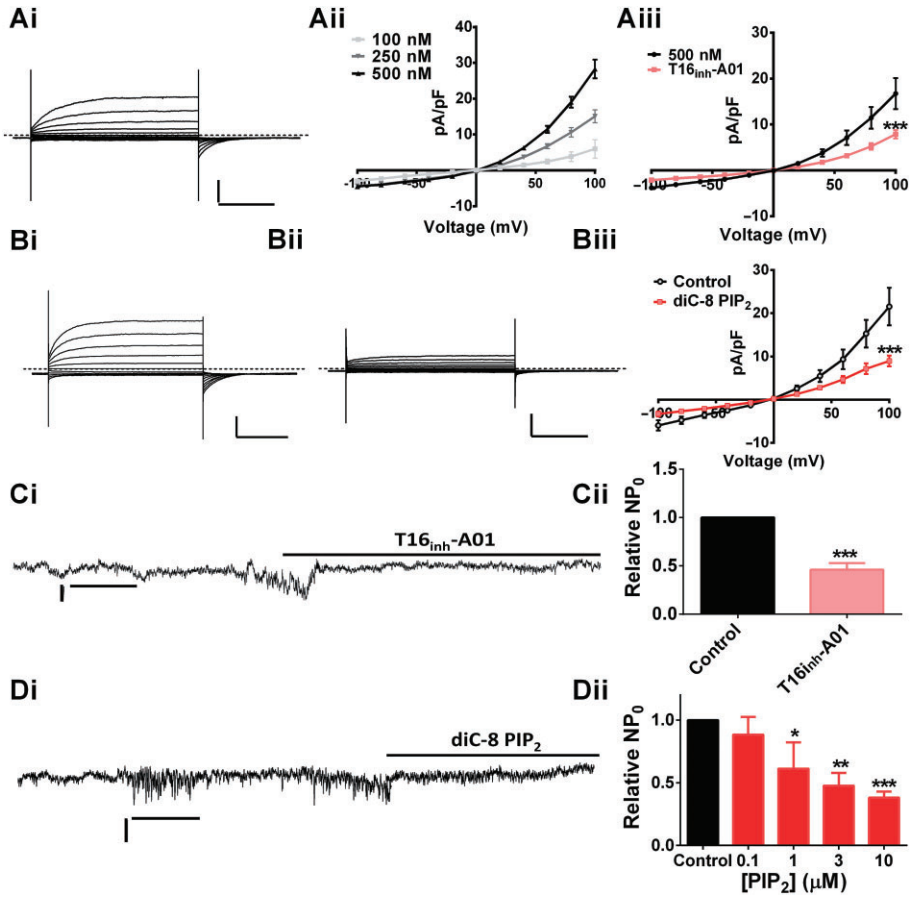

Figure 2

Enrichment of PASMC with diC-8 PI(4,5)P_2 attenuated I_{ClCa}. (Ai) Representative I_{ClCa} activated by 500 nM [Ca^{2+}] within the pipette solution from −100 to +100 mV. (Aii) shows the mean currents evoked using pipette solutions containing different [Ca^{2+}] (n = 4–7). (Aiii) Currents elicited by 500 nM free Ca^{2+} in the absence (black) and presence of 10 μM T16$_{inh}$-A01 (pink, ***P < 0.001). (Bi and Bii) Currents evoked by 500 nM free Ca^{2+} alone or after inclusion of 1 μM diC-8 PI(4,5)P_2 (Bii). Mean data are shown in (Biii) (n = 7, ***P < 0.001). Whole cell horizontal bars and vertical bars represent 20 pA·pF^{-1} and 500 ms. Dashed line represents zero current level. (C) Inside-out excised patches activated by 500 nM free [Ca^{2+}] that were sensitive to 10 μM T16$_{inh}$-A01 (Cii shows mean data, n = 5, ***P < 0.001). (Di) Representative effect of 10 μM diC-PI(4,5)P_2 on excised patches and the concentration-dependence of the inhibitory effect of diC-PI(4,5)P_2 (100 nM–10 μM) is shown in (Dii) (n = 4–8, *P < 0.05, **P < 0.01, ***P < 0.001). Single channel horizontal bars and vertical bars represent 0.2 pA and 20 s.

observed in our previous study (Davis *et al.*, 2013). Enriching whole cell pipette solutions with 1 μM diC-8 PI(4,5)P_2, a water-soluble form of PI(4,5)P_2, attenuated whole cell I_{ClCa} compared to same-day controls, (Figure 2B; n = 7, P < 0.001). I_{ClCa} generated in cells isolated using a more acute method were also sensitive to 1 μM diC-8 PI(4,5)P_2 (8.17 ± 2.4 pA·pF^{-1} vs. 17.1 ± 2.3 pA·pF^{-1}, in same-day controls P < 0.001, n = 5) (see Supporting Information Fig. S1). To determine the concentration-dependence of this effect, we studied a range of [diC-8 PI(4,5)P_2] on single channel I_{ClCa}. Application of a bathing solution containing 500 nM free [Ca^{2+}] resulted in robust, low amplitude channel activity similar to previous studies (Piper and Large, 2003; Davis *et al.*, 2013), which was inhibited considerably by application of 10 μM T16$_{inh}$-A01 (Figure 2C; n = 5, P < 0.01). Application of diC-8 PI(4,5)P_2 (100 nM–10 μM) to the cytosolic surface of excised patches, inhibited I_{ClCa}, with 1 μM producing approximately 0% reduction (Figure 2Dii). The maximum inhibition of I_{ClCa} *by* diC-8 PI(4,5)P_2 was similar to that produced by 10 μM T16$_{inh}$-A01 (Figure 2Di).

Depletion of endogenous PI(4,5)P_2 augments I_{ClCa}

Intracellular enrichment of PI(4,5)P_2 attenuated I_{ClCa} so we postulated that depletion of PI(4,5)P_2 levels would augment I_{ClCa}. Wortmannin, at high concentrations, is a PI4K inhibitor, therefore preventing the synthesis of PI(4,5)P_2 and depleting cellular PI(4,5)P_2 levels (Saleh *et al.*, 2009). Pretreating PASMC for 1 h with 20 μM wortmannin resulted in currents evoked by 500 nM Ca^{2+}-containing pipette solutions that were considerably larger than same-day controls (Figure 3Ai,Aiii; n = 9, P < 0.001). Application of the α_1-adrenoceptor agonist methoxamine to cells incubated in wortmannin produced a further marked increase in current amplitude (Figure 3Aiii; n = 4, P < 0.001) within 5 min. Finally, α-cyclodextrin (α-CD) (3 mg·mL^{-1}), a cell permeable phospholipid acceptor,

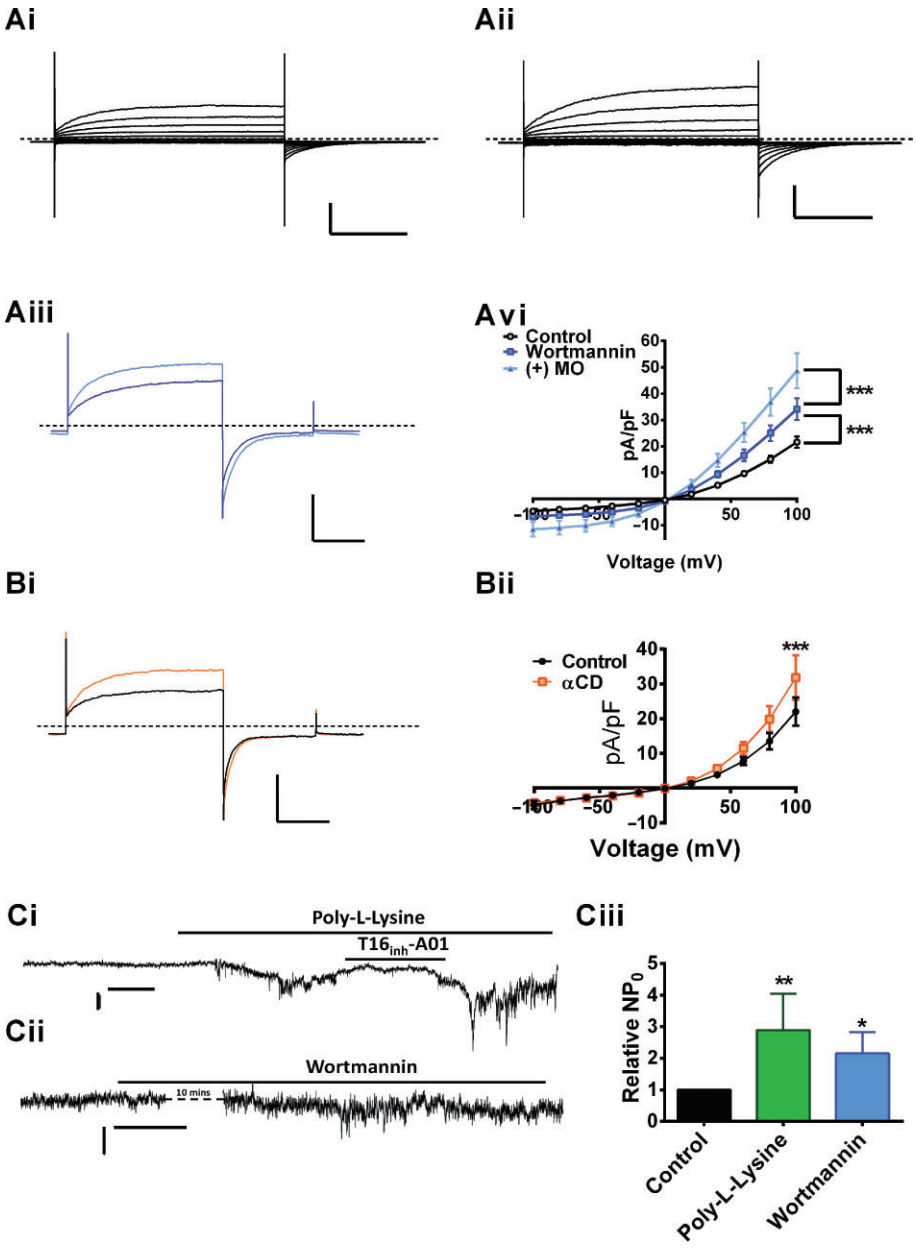

Figure 3

Inhibition of PI(4,5)P_2 synthesis and removal of PI(4,5)P_2 augments I_{ClCa}. Pretreatment of PASMC with wortmannin augmented I_{ClCa} (Aii) compared to same-day controls (Ai, $n = 9$, ***$P < 0.001$). Further application of 1 μM methoxamine (MO) augmented I_{ClCa} in 20 μM wortmannin-treated cells significantly (Aiii, $n = 4$, $P < 0.001$). Whole cell horizontal bars and vertical bars represent 20 pA·pF^{-1} and 500 ms. (B) Application of 3 mg·mL^{-1} αCD also augmented I_{ClCa}, within 5 min (B, $n = 5$, ***$P < 0.001$). Horizontal and vertical scale bars represent 500 ms and 200 pA, respectively, dashed line represents 0 pA. (Ci) Application of 50 μg·L^{-1} poly-L-lysine increased I_{ClCa} in excised patches, which was attenuated by subsequent application of 10 μM T16$_{inh}$-A01 ($n = 5$). I_{ClCa} was also augmented by the application of 20 μM wortmannin. (Ciii) The mean relative NP_0 for currents activated by 500 nM Ca^{2+} under control conditions and in the presence of poly-L-lysine ($n = 9$, **$P < 0.01$) and 20 μM wortmannin ($n = 6$, *$P < 0.05$). Single channel horizontal bars and vertical bars represent 0.2 pA and 20 s.

increased I_{ClCa} within 5 min in cells isolated using both the overnight dispersal (Figure 3B; $n = 5$, $P < 0.001$) and acute method (7.04 ± 0.8 pA·pF^{-1} vs. 9.55 ± 0.5 pA·pF^{-1} at +70 mV; see Supporting information Fig. S1). In single channel experiments, a known PI(4,5)P_2 scavenger, poly-L-lysine (50 μg·mL^{-1}) augmented I_{ClCa} markedly (Figure 3Ci; $n = 9$, $P < 0.01$); this effect was attenuated reversibly by application of 10 μM T16$_{inh}$-A01 (Figure 4Ci; $n = 5$). Application of wortmannin for 10 min also increased single channel activity with the NP_o increased by twofold (Figure 3Cii; $n = 6$, $P < 0.05$).

PLC inhibition attenuates I_{ClCa}

Having shown that modulation of PI(4,5)P_2 levels altered I_{ClCa} activity, we then looked at whether PI(4,5)P_2 hydrolysis was

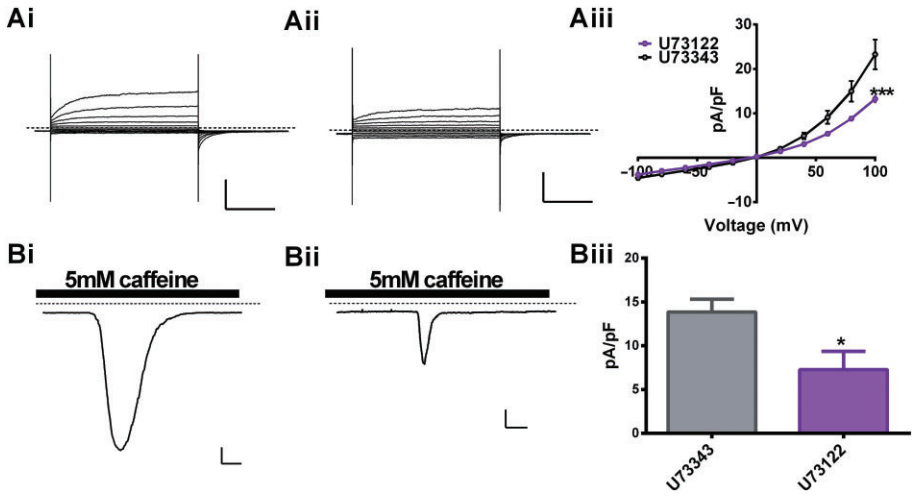

Figure 4

Phospholipase C inhibition attenuated I_{ClCa}. (Representative I_{ClCa} evoked in PA cells incubated in 2 μM U73343 (Ai) or 2 μM U73122 (Aii) and the mean data are shown in (Aiii) with same-day control (Ai) (n = 7, ***P < 0.001). I–V horizontal bars and vertical bars represent 20 pA·pF^{-1} and 500 ms. (B) Representative currents recorded with the perforated patch configuration after application of 5 mM caffeine in the presence of U73433 (Bi) or U73122 (Bii) for 10 min. Mean data for four such experiments are shown in (Biii, *P < 0.05). Perforated patch horizontal bars and vertical bars represent 2 pA·pF^{-1} and 2 s. Dashed line represents 0 pA.

obligatory for CACC gating *per se*. To do this, we utilized two different, Gq independent methods to elicit I_{ClCa} that should theoretically not involve PLC activation. Pipette solutions containing 500 nM free [Ca^{2+}] generated I_{ClCa} that were attenuated by ~45% after 10 min of incubation with the PLC inhibitor U77312 (2 μM) compared to the inactive analogue U77343 (2 μM) (Figure 4A; n = 6, P < 0.001). In perforated patch recordings, 5 mM caffeine was used to activated ryanodine receptors and increase intracellular Ca^{2+}. This produced robust, transient inward currents at –50 mV that were attenuated by $T16_{inh}$-A01 and were also sensitive to and reduced by ~50% on incubation with U73122 (Figure 4B, n = 4, P < 0.05). These data suggest that removal of PI(4,5)P_2 may contribute to the inherent gating mechanism of CaCCs in rat PA smooth muscle cells.

Discussion

The present study shows for the first time that PI(4,5)P_2 plays an inhibitory role in native CaCC activity. This is based upon many lines of evidence. (i) Agents that reduce PI(4,5)P_2 levels through different routes [PLC activation, PI4K inhibition, PI(4,5)P_2 scavenging and absorption], all increased I_{ClCa} evoked by solutions containing clamped-free [Ca^{2+}]. (ii) Enrichment of activating solutions with PI(4,5)P_2 inhibited I_{ClCa} in PA smooth muscle cells. (iii) PI(4,5)P_2 and other phospholipids were shown to bind directly to TMEM16A isolated from whole PA and TMEM16A-eGFP expressed in HEK cells. The caveats of these studies were that the reagents used indirectly modulate PI(4,5)P_2 levels and are likely to alter other intracellular signals. More precise depletion via voltage-sensitive phosphatases used in heterologous expression systems (Falkenburger *et al.*, 2010) would be desirable, but the fact that reagents that alter PI(4,5)P_2 through very different mechanisms all produced similar enhancements of the I_{ClCa} and supplementation with diC-8 PI(4,5)P_2 had opposite effects adds considerable weight to the view that PI(4,5)P_2 suppresses CaCC activity. Consequently, localized hydrolysis of this phospholipid within the proximity of the CaCC may be vital for channel activity. The majority of other ion channels regulated by PI(4,5)P_2 are stimulated by the phosphoinositide (Suh and Hille, 2008), so the 'inverted sensitivity' shown by CaCCs in rat PA is a relatively rare observation. Before this investigation, no interaction of a native CaCC with a phosphoinositide has been shown except for Ins(3,4,5,6)P_4-mediated inhibition of a CaMKII-stimulated CaCC in epithelial cells (Xie *et al.*, 1996) and stimulation of TMEM16A currents by two synthetic inositol tetrakisphosphates (Tian *et al.*, 2013). The latter study showed no effect of wortmannin on I_{ClCa} in HEK293 cells transfected with TMEM16A, in contrast to our observed binding of TMEM16A-eGFP to concentrated phosphoinositides in 'PIP strips'. Interestingly, our studies showed that there was no difference in dot blot signals between untransfected HEK293 cells and ones transfected with TMEM16A, consistent with PI(4,5)P_2 binding saturating with the endogenous TMEM16A. Consequently, in overexpression studies, the low composition of PI(4,5)P_2 in the cell membrane (2%) cannot modulate the high concentration of heterologously expressed TMEM16A protein.

Bioinformatics analysis revealed many potential candidates for PI(4,5)P_2 binding sites within the mouse TMEM16A sequence (Figure 5). Being negatively charged, PIP_2 would have a favourable interaction for basic residues loosely interspersed by hydrophobic residues. Based upon homology mapping with the KRWRK sequence on TRPV4, which is the PI(4,5)P_2 binding site required for channel activation (Garcia-Elias *et al.*, 2013), a PI(4,5)P_2 binding motif (KRFRR) is

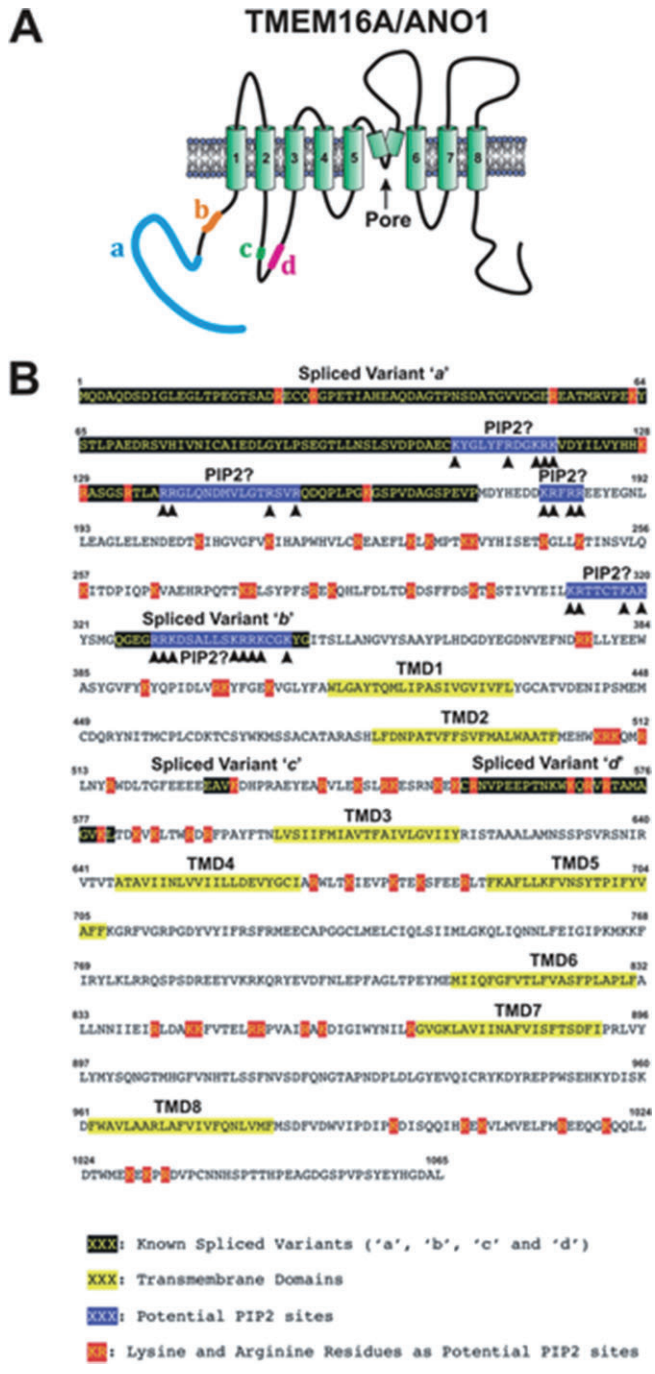

Figure 5

Putative PIP_2 binding sites in the mouse TMEM16A full sequence (1065 amino acid; MW: 122 kDa). (A) The predicted secondary structure of the TMEM16A/ANO1 protein. The model highlights the eight transmembrane domains (TMDs), the speculated pore region lying between TMD5 and TMD6, and the position of the four known spliced variants labelled '*a*', '*b*', '*c*' and '*d*'. (B) The full mouse TMEM16A sequence including the four spliced variants, the eight transmembrane domains and sequences (highlighted in blue) that are homologous to sequences previously shown to interact with PIP_2 and modulate ion channel activity such as pleckstrin homology (PH) domains (Suh and Hille, 2008) or one recently shown to specifically regulate TRPV4 channels (TRPV4: KRWRK; TMEM16A: K_{181}RFRR$_{185}$) (Garcia-Elias *et al.*, 2013). Numbers above the sequence indicate amino acid number from the C to the N terminus. Arrows in highlighted candidate PIP_2 sequences show the position of arginine (R) and lysine (K) residues. Other R and K residues in all cytoplasmic domains that could potentially represent PIP_2 binding sites are also highlighted.

located just after the 'a' splice variant domain of TMEM16A (see Figure 5). There is also a potential binding site within the 'b' splice variant region, which is known to greatly reduce Ca^{2+} sensitivity of TMEM16A (Ferrera *et al.*, 2009). Consequently, the suppressive effect of this splice variant may reflect an inhibitory role of $PI(4,5)P_2$ rather than direct Ca^{2+} binding (Ferrera *et al.*, 2009). While it is beyond the scope of the present study, it will be the focus of future studies to define precisely the molecular architecture of the $PI(4,5)P_2$ binding site on the TMEM16A protein.

The present study showed that $PI(4,5)P_2$, as low as 1 μM, had a marked effect on I_{ClCa} in rat PA smooth muscle cells. This sensitivity is considerably higher than most other ion channels studied. For instance, KCNQ-encoded, voltage-gated K_v7 channels are enhanced by $PI(4,5)P_2$ with EC_{50}s of 2.6–215 μM for KCNQ2, KCNQ3, KCNQ2/3 heteromers and KCNQ4 (Li *et al.*, 2004; Hernandez *et al.*, 2008). In CHO cells, overexpressed KCNQ2 and KCNQ3 homomeric channels have EC_{50}s of 205 and 2.6 μM, respectively, and the KCNQ2/3 heteromer EC_{50} of 40 μM (Li *et al.*, 2005). $PI(4,5)P_2$ was also required for activation of endogenous TRPC1 in vascular smooth muscle cells with an EC_{50} of 1–3 μM (Saleh *et al.*, 2009). The $[PI(4,5)P_2]$ of mammalian cells is purported to be ~ 10–210 μM (McLaughlin *et al.*, 2002; Winks *et al.*, 2005), which would result in complete suppression of CaCCs in arterial smooth muscle. Therefore, either $[PI(4,5)P_2]$ close to CaCCs is lower than a theoretical bulk concentration or there are local signalling complexes that modulate $[PI(4,5)P_2]$ in the proximity of the channel. Previous studies have proposed that TMEM16A proteins reside in lipid raft components of the plasma membrane in vascular smooth muscle (Sones *et al.*, 2010) and dorsal root ganglia (Jin *et al.*, 2013). Our finding that inhibition of PLC reduced the amplitude of I_{ClCa} evoked by either caffeine or internal perfusion with pipette solutions of known free $[Ca^{2+}]$, that do not involve IP_3 generation, suggests that removal of $PI(4,5)P_2$ suppression may be a fundamental aspect in CaCC gating and may even represent an alternative activation mechanism (see Figure 6). This also raises the possibility of different pools of $PI(4,5)P_2$ and/or PLC isoforms, which are separate from those associated with Gq protein-coupled receptors. Furthermore, our experiments with proprietary phospholipid assays or 'PIP strips' revealed that it was not just PIP_2 but all forms of phosphoinositide that interacted with TMEM16A. The effect of these other phosphoinositides on endogenous CaCCs will be the focus of future studies, but these findings suggest that regulation of CaCC activity in vascular smooth muscle is likely to be complex and multifactorial.

It is now generally accepted that TMEM16A expression products contribute to native CaCCs in different cell types.

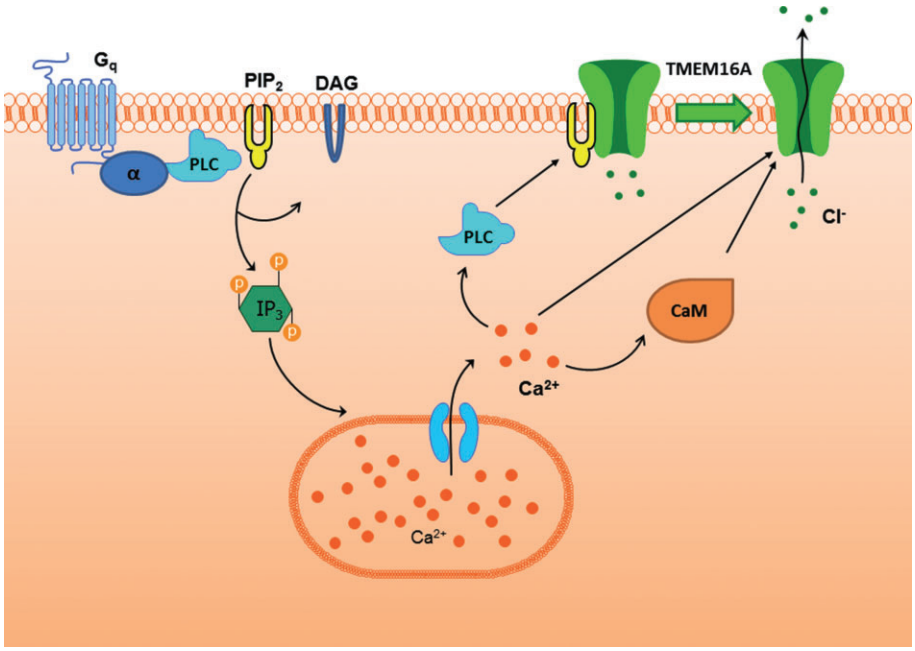

Figure 6

Role of PI(4,5)P2 in TMEM16A regulation. The schematic diagram shows the classical role of PIP_2 as a substrate for PLC in the production of diacylglycerol (DAG) and inositol trisphosphate (IP_3) via Gq activation pathway. This will lead to an increase in intracellular [Ca^{2+}], which is known to activate TMEM16A. However, we have shown that PI(4,5)P_2 is also bound to TMEM16A at rest and subsequently removed when the channel is activated. Therefore, we propose that the increase in intracellular [Ca^{2+}] has two important effects on TMEM16A activity: (i) activates PLC to remove PI(4,5)P_2 bound to TMEM16A and (ii) activates the channel either directly or indirectly via calmodulin (CaM).

However, there are conflicting ideas about the Ca^{2+}-dependent gating mechanism of these channels as there is not a well-established Ca^{2+} binding site on TMEM16A. Some groups have identified putative Ca^{2+} binding sites in the first intracellular loop (Xiao *et al.*, 2011), N-terminus (Ferrera *et al.*, 2009) or in TM6-7 intracellular loop (Terashima *et al.*, 2013), whereas others suggest that channel activity is regulated by the binding of Ca^{2+}-calmodulin complex (Tian *et al.*, 2011; Jung *et al.*, 2013; Vocke *et al.*, 2013). It is well established in KCNQ (Delmas and Brown, 2005) and TRPC (Kwon *et al.*, 2007) channels that PI(4,5)P_2 and calmodulin play reciprocal roles in channel activity and potentially bind at the same site. If a similar situation exists for TMEM16A, then the debate over the gating of these channels may reflect a variable binding of PI(4,5)P_2 that needs to be removed and potentially be replaced by Ca^{2+}-calmodulin. This, in turn, either activates the channel or allows Ca^{2+} to gate the channel directly. Overall, our data reveal that CaCC activity, certainly in vascular smooth muscle cells, is restrained by a phosphoinositide 'brake', and membrane receptor agonists not only provide the trigger for Ca^{2+}, but also allow CaCC activation through PI(4,5)P_2 hydrolysis.

Acknowledgements

The original non-eGFP-tagged TMEM16A mouse clone was a kind gift from Professor Lily Jan, University of California, San Francisco. Protein samples from a TMEM16A knockout mouse were kindly provided by Professor Karl Kunzelmann, University of Regensburg, Germany.

Author contributions

H. A. T. P.: Acquisition of data, analysis and interpretation of data, and drafting of the manuscript.

N. L., A. P. A. and I. A. G.: Analysis and interpretation of data and drafting of the manuscript.

Conflicts of interest

None.

References

Alexander SPH, Benson HE, Faccenda E, Pawson AJ, Sharman JL, Spedding M, Peters JA and Harmar AJ, CGTP Collaborators. (2013) The Concise Guide to PHARMACOLOGY 2013/14: Ion channels. Br J Pharmacol 170: 1607–1651.

Angermann JE, Sanguinetti AR, Kenyon JL, Leblanc N, Greenwood IA (2006). Mechanism of the inhibition of Ca^{2+}-activated Cl^- currents by phosphorylation in pulmonary arterial smooth muscle cells. J Gen Physiol 128: 73–87.

Barroso-González J, Machado JD, García-Expósito L, Valenzuela-Fernández A (2009). Moesin regulates the trafficking of nascent clathrin-coated vesicles. J Biol Chem 284: 2419–2434.

Bulley S, Neeb ZP, Burris SK, Bannister JP, Thomas-Gatewood CM, Jangsangthong W *et al*. (2012). TMEM16A/ANO1 channels contribute to the myogenic response in cerebral arteries. Circ Res 111: 1027–1036.

Caputo A, Caci E, Ferrera L, Pedemonte N, Barsanti C, Sondo E *et al*. (2008). TMEM16A, a membrane protein associated with calcium-dependent chloride channel activity. Science 322: 590–594.

Chipperfield AR, Harper AA (2000). Chloride in smooth muscle. Prog Biophys Mol Biol 74: 175–221.

Criddle DN, de Moura RS, Greenwood IA, Large WA (1996). Effect of niflumic acid on noradrenaline-induced contractions of the rat aorta. Br J Pharmacol 118: 1065–1071.

Dam VS, Boedtkjer DM, Nyvad J, Aalkjaer C, Matchkov V (2013). TMEM16A knockdown abrogates two different Ca(2+)-activated Cl (–) currents and contractility of smooth muscle in rat mesenteric small arteries. Pflugers Arch. doi: 10.1007/S00424-013-1382-1.

Davis AJ, Forrest AS, Jepps TA, Valencik ML, Wiwchar M, Singer CA *et al*. (2010). Expression profile and protein translation of TMEM16A in murine smooth muscle. Am J Physiol Cell Physiol 299: C948–C959.

Davis AJ, Shi J, Pritchard HA, Chadha PS, Leblanc N, Vasilikostas G *et al*. (2013). Potent vasorelaxant activity of the TMEM16A inhibitor T16A(inh) -A01. Br J Pharmacol 168: 773–784.

Delmas P, Brown DA (2005). Pathways modulating neural KCNQ/M (Kv7) potassium channels. Nat Rev Neurosci 6: 850–862.

Falkenburger BH, Jensen JB, Hille B (2010). Kinetics of PIP2 metabolism and KCNQ2/3 channel regulation studied with a voltage-sensitive phosphatase in living cells. J Gen Physiol 135: 99–114.

Ferrera L, Caputo A, Ubby I, Bussani E, Zegarra-Moran O, Ravazzolo R *et al*. (2009). Regulation of TMEM16A chloride channel properties by alternative splicing. J Biol Chem 284: 33360–33368.

Forrest AS, Joyce TC, Huebner ML, Ayon RJ, Wiwchar M, Joyce J *et al*. (2012). Increased TMEM16A-encoded calcium-activated chloride channel activity is associated with pulmonary hypertension. Am J Physiol Cell Physiol 303: C1229–C1243.

Garcia-Elias A, Mrkonjic S, Pardo-Pastor C, Inada H, Hellmich UA, Rubio-Moscardó F *et al*. (2013). Phosphatidylinositol-4,5-biphosphate-dependent rearrangement of TRPV4 cytosolic tails enables channel activation by physiological stimuli. PNAS 110: 9553–9558.

Greenwood IA, Ledoux J, Leblanc N (2001). Differential regulation of Ca(2+)-activated Cl(–) currents in rabbit arterial and portal vein smooth muscle cells by Ca(2+)-calmodulin-dependent kinase. J Physiol 534: 395–408.

Heinze C, Seniuk A, Sokolov MV, Huebner AK, Klementowicz AE, Szijártó IA *et al*. (2014). Disruption of vascular Ca^{2+}-activated chloride currents lowers blood pressure. J Clin Invest 124: 675–686.

Hernandez CC, Zaika O, Tolstykh GP, Shapiro MS (2008). Regulation of neural KCNQ channels: signalling pathways, structural motifs and functional implications. J Physiol 586: 1811–1821.

Jin X, Shah S, Liu Y, Zhang H, Lees M, Fu Z *et al*. (2013). Activation of the Cl^- channel ANO1 by localized calcium signals in nociceptive sensory neurons requires coupling with the IP3 receptor. Sci Signal 6: ra73.

Jung J, Nam JH, Park HW, Oh U, Yoon JH, Lee MG (2013). Dynamic modulation of ANO1/TMEM16A HCO3(-) permeability by Ca^{2+}/calmodulin. PNAS U S A 110: 360–365.

Kwon Y, Hofmann T, Montell C (2007). Integration of phosphoinositide- and calmodulin-mediated regulation of TRPC6. Mol Cell 25: 491–493.

Li Y, Gamper N, Shapiro MS (2004). Single-channel analysis of KCNQ K^+ channels reveals the mechanism of augmentation by a cysteine-modifying reagent. J Neurosci 24: 5079–5090.

Li Y, Gamper N, Hilgemann DW, Shapiro MS (2005). Regulation of Kv7 (KCNQ) K^+ channel open probability by phosphatidylinositol 4,5-bisphosphate. J Neurosci 25: 9825–9835.

Manoury B, Tamuleviciute A, Tammaro P (2010). TMEM16A/anoctamin 1 protein mediates calcium-activated chloride currents in pulmonary arterial smooth muscle cells. J Physiol 588 (Pt 13): 2305–2314.

McLaughlin S, Wang J, Gambhir A, Murray D (2002). PIP(2) and proteins: interactions, organization, and information flow. Annu Rev Biophys Biomol Struct 31: 151–175.

Piper AS, Large WA (2003). Multiple conductance states of single Ca^{2+}-activated Cl^- channels in rabbit pulmonary artery smooth muscle cells. J Physiol 547: 181–196.

Saleh SN, Albert AP, Large WA (2009). Obligatory role for phosphatidylinositol 4,5-bisphosphate in activation of native TRPC1 store-operated channels in vascular myocytes. J Physiol 587 (Pt 3): 531–540.

Schroeder BC, Cheng T, Jan YN, Jan LY (2008). Expression cloning of TMEM16A as a calcium-activated chloride channel subunit. Cell 134: 1019–1029.

Shi J, Birnbaumer L, Large WA, Albert AP (2014). Myristoylated alanine-rich C kinase substrate coordinates native TRPC1 channel activation by phosphatidylinositol 4,5-bisphosphate and protein kinase C in vascular smooth muscle. FASEB J 28: 244–255.

Sones WR, Davis AJ, Leblanc N, Greenwood IA (2010). Cholesterol depletion alters amplitude and pharmacology of vascular calcium-activated chloride channels. Cardiovasc Res 87: 476–484.

Suh BC, Hille B (2008). PIP2 is a necessary cofactor for ion channel function: how and why? Annu Rev Biophys 37: 175–195.

Sun H, Xia Y, Paudel O, Yang XR, Sham JS (2012). Chronic hypoxia-induced upregulation of Ca^{2+}-activated Cl^- channel in pulmonary arterial myocytes: a mechanism contributing to enhanced vasoreactivity. J Physiol 590: 3507–3521.

Terashima H, Picollo A, Accardi A (2013). Purified TMEM16A is sufficient to form Ca^{2+}-activated Cl^- channels. PNAS U S A 110: 19354–19359.

Thomas-Gatewood C, Neeb ZP, Bulley S, Adebiyi A, Bannister JP, Leo MD *et al*. (2011). TMEM16A channels generate Ca^{2+}-activated Cl^- currents in cerebral artery smooth muscle cells. Am J Physiol Heart Circ Physiol 301: H1819–H1827.

Tian Y, Kongsuphol P, Hug M, Ousingsawat J, Witzgall R, Schreiber R *et al*. (2011). Calmodulin-dependent activation of the epithelial calcium-dependent chloride channel TMEM16A. FASEB J 25: 1058–1068.

Tian Y, Schreiber R, Wanitchakool P, Kongsuphol P, Sousa M, Uliyakina I *et al*. (2013). Control of TMEM16A by INO-4995 and other inositolphosphates. Br J Pharmacol 168: 253–265.

Vocke K, Dauner K, Hahn A, Ulbrich A, Broecker J, Keller S *et al*. (2013). Calmodulin-dependent activation and inactivation of

anoctamin calcium-gated chloride channels. J Gen Physiol 142: 381–404.

Wang M, Yang H, Zheng LY, Zhang Z, Tang YB, Wang GL *et al.* (2012). Downregulation of TMEM16A calcium-activated chloride channel contributes to cerebrovascular remodeling during hypertension by promoting basilar smooth muscle cell proliferation. Circulation 125: 697–707.

Winks JS, Hughes S, Filippov AK, Tatulian L, Abogadie FC, Brown DA *et al.* (2005). Relationship between membrane phosphatidylinositol-4,5-bisphosphate and receptor-mediated inhibition of native neuronal M channels. J Neurosci 25: 3400–3413.

Xiao Q, Yu K, Perez-Cornejo P, Cui Y, Arreola J, Hartzell HC (2011). Voltage- and calcium-dependent gating of TMEM16A/Ano1 chloride channels are physically coupled by the first intracellular loop. Proc Natl Acad Sci U S A 108: 8891–8896.

Xie W, Kaetzel MA, Bruzik KS, Dedman JR, Shears SB, Nelson DJ (1996). Inositol 3,4,5,6-tetrakisphosphate inhibits the calmodulin-dependent protein kinase II-activated chloride conductance in T84 colonic epithelial cells. J Biol Chem 271: 14092–14097.

Yamazaki J, Kitamura K (2001). Cell-to-cell communication via nitric oxide modulation of oscillatory Cl(–) currents in rat intact cerebral arterioles. J Physiol 536: 67–78.

Yang YD, Cho H, Koo JY, Tak MH, Cho Y, Shim WS *et al.* (2008). TMEM16A confers receptor-activated calcium-dependent chloride conductance. Nature 455: 1210–1215.

Supporting information

Additional Supporting Information may be found in the online version of this article at the publisher's web-site:

http://dx.doi.org/10.1111/bph.12778

Figure S1 Acute dispersal of rPASMC is also sensitive to PI(4,5)P_2. (A) I_{ClCa} was attenuated with inclusion of 1 μM PI(4,5)P_2 (Aii) compared to same-day controls (Ai), with mean *I–V* shown (Aii, n = 5). (B) Application of 3 mg·mL^{-1} α-cyclodextrin (orange) increased I_{ClCa} after 5 min application, with mean data shown at +70 mV (n = 5).